Multi-polarized Reconfigurable Antenna with Ground Plane Slot and Capacitance Feeding for UAV-to-everything Communications

Seong-Hyeop Ahn[1], Yu-Seong Choi[2], Mohamed Elhefnawy[1,3], and Wang-Sang Lee[1]

[1]Department of Electrical Engineering, Gyeongsang National University (GNU)
B405-401501, Jinju-daero, Jinju-si Gyeongnam, 52828, Republic of Korea
dksak2115@gnu.ac.kr, wsang@gnu.ac.kr

[2]Korea Aerospace Industries (KAI), Ltd
78, Gongdan 1-ro, Sanam-myeon, Sacheon-si
Gyeongnam, 52529, Republic of Korea

[3]Department of Electrical Engineering
Faculty of Engineering, October 6 University, Egypt
mmmelhefnawy.eng@o6u.edu.eg

Abstract – This paper proposes a polarized reconfigurable antenna for unmanned aerial vehicles (UAVs) with flexible UAV-to-Everything (U2X) communications through a reduction of polarization loss. It operates at 2.45 GHz and consists of a square patch antenna, a capacitance feed, a ground surface slot, and a reconfigurable feeding network. The reconfigurable feeding network has dual polarization (linear, circular) depending on the configuration of the feeding network. The dual linear polarization reconfigurable feeding network configuration consists of a single-pole double-throw (SPDT) switch, a 50-ohm microstrip line, and a low-temperature co-fired ceramic (LTCC) 90-degree hybrid coupler. This was added to the circuit to form a double circular polarization reconfigurable feeding network. The proposed antenna has a miniaturized size $(0.389\lambda_o \times 0.389\lambda_o \times 0.005\lambda_o)$, and is lightweight (12.2 g), making it suitable for low-height flight. Furthermore, it has maximum gains of 6.6 dBi and 7.2 dBi, in addition to an efficiency of 82%, and a 10 dB bandwidth of 4.5% (2.38-2.49 GHz). Therefore, the proposed antenna covers all UAV control links, video, and telemetry frequency bands (2.38-2.485 GHz).

Index Terms – Capacitance feed, ground surface slot, polarization-reconfigurable antenna, UAV-to-Everything communications.

I. INTRODUCTION

The unmanned aerial vehicles (UAVs) industry, one of the core challenges of the Fourth Industrial Revolution, has high marketability and economic value. It is expected to grow by $21.8 billion by 2027, based on the benefits of its applications in various fields such as surveillance/research, hobby/leisure, imaging, and life-saving [1]. Based on these values, research and development of communication platforms for UAVs are also rapidly growing and changing in line with this. Unlike conventional terrestrial wireless communication environments, the UAV communication environment has specific requirements for operation at a certain altitude, so it must be accompanied by flexible UAV-to-Everything (U2X) communication technology that can perform various tasks in different ways. Therefore, the implementation of an antenna with multiple polarizations is essential to reduce polarization loss. The antennas for U2X communications should have many characteristics, including compact size, low profile, and light weight. Additionally, they should cover the frequency band for UAV communication. There have been many research papers focused on the design of antennas for unmanned aerial vehicles. For example, single-polarized antennas without reconfigurability have been studied in [2–4]. The use of single-polarized antennas with U2X communication systems could degrade their performance due to cross-polarization loss. Accordingly, research on polarization-reconfigurable antennas is continuing to reduce polarization losses in wireless communication systems [5–6]. The polarization-reconfigurable antenna has a good gain and impedance bandwidth performance, despite being relatively large in size [7–11]. For the miniaturization of the antenna, a patch antenna with a slot was used in [12–13]. But [12] and [13] have a narrow bandwidth of approximately 7%. In [14–15], researchers have studied a meta-surface antenna that can rotate mechanically and a ring slot antenna that offers

both linear and circular polarization. The meta-surface antenna in [14] has a large size but provides wide bandwidth and high gain. On the other hand, the ring slot antenna in [15] has a small size and wide bandwidth, but it has low gain. In [16], the reconfigurable patch antenna with PIN diodes has both linear and circular polarization but the antenna has narrow impedance and axial ratio bandwidths. [17] investigated the design of an antenna that includes four parasitic patches and two varactor diodes on each patch. By reconfiguring this antenna, it is possible to achieve dual polarization with two beams for each polarization. However, manufacturing this antenna is challenging due to its complex structure, and integrating it as an aerodynamic component to be attached to UAVs is difficult.

In this paper, we propose a compact, multi-polarized, reconfigurable patch antenna that covers the frequency band for unmanned aerial vehicle communication.

II. PROPOSED MULTI-POLARIZED PATCH ANTENNA

Figure 1 (a) shows a schematic diagram of the overall structure and feeding of the proposed antenna. A patch antenna is placed on the top surface of the upper substrate, and a capacitance power supply unit for power supply and impedance matching is located below it. By changing the length and width of the capacitance feeding part, the series capacitance can be adjusted to achieve impedance matching. The antenna is designed to operate at 2.45 GHz for WLAN applications. The proposed antenna was fabricated using an RF-60TC substrate from Taconic, which has a thickness of 0.64 mm. The dielectric constant (ε_r) is 6.15 and the loss tangent ($\tan\delta$) is 0.002. On the top surface of the lower substrate, slots are arranged at four corners for impedance matching, front-to-back ratio improvement, and wide electrical length, even in small ground surface sizes. The air gap between the upper and lower substrates is connected through the fixed pins and the feeding pins. It is designed to connect the signal from the power supply circuit to the capacitance power supply. As shown in Figs. 1 (b)-(c), the antenna structure has the following layout parameters: the width of the substrate (W_s) is 49 mm, the width of the square patch (W_p) is 37.5 mm, the width (W_{pin}) and height (H_{pin}) of the feeding and fixed pins are 10 mm and 5 mm, respectively, the distance (W_g) between the patch and feed pin is 2.25 mm, slot width (S_w) is 2 mm, slot length (S_l) is 20 mm, length from corner to the slot (S_m) is 3 mm, linear polarization (LP) feed line length (L_{f1}) and circular polarization (CP) feed line length (L_{f2}) are x mm and y mm, capacitance feed line width (W_c) and length (L_c) are 1 mm and 2.75 mm, respectively. The overall size of the proposed multi-polarized antenna
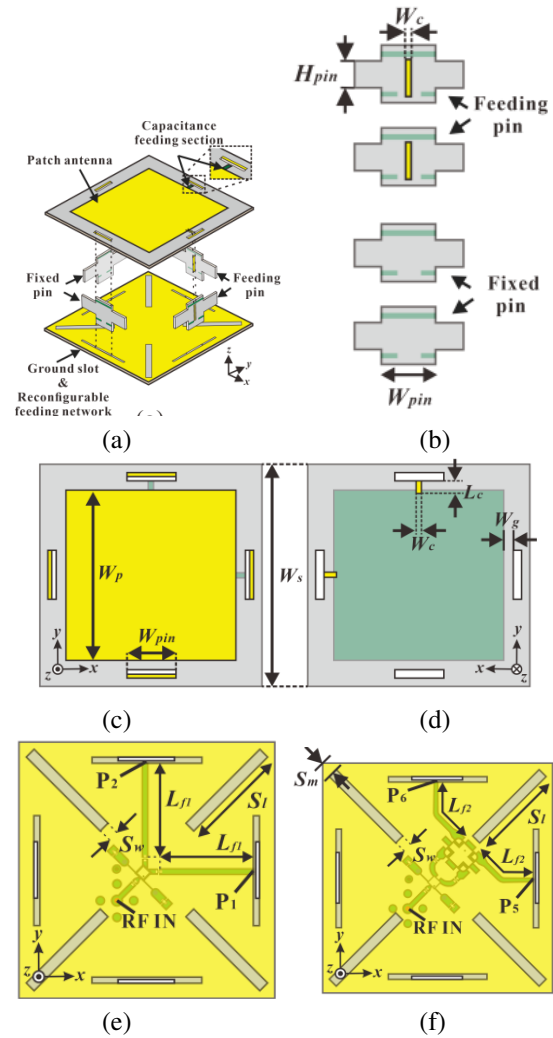

Fig. 1. Proposed antenna configuration: (a) Overall configurations of the proposed patch antenna, (b) front views of fixed and feeding pins, (c)-(d) top and bottom views of the upper substrates, and (e)-(f) top views of the feeding network that forms linear polarization and circular polarization.

is ($0.389\lambda_o \times 0.389\lambda_o \times 0.005\lambda_o$), where λ_o is the wavelength in free space at the lowest frequency of operation (2.38 GHz). For the miniaturization of the proposed multi-polarized antenna, the patch antenna was designed to be miniaturized using the slot on the ground plane, as shown in Fig. 1 (d).

The electrical length was increased through the effect of the meander line, as the current flow was changed by the arrangement of slots at each corner of the ground plane. To obtain the optimum structure for the proposed antenna, the parameter sweep and optimization tools of the CST Microwave Studio 2022 have been used to determine the optimized dimensions
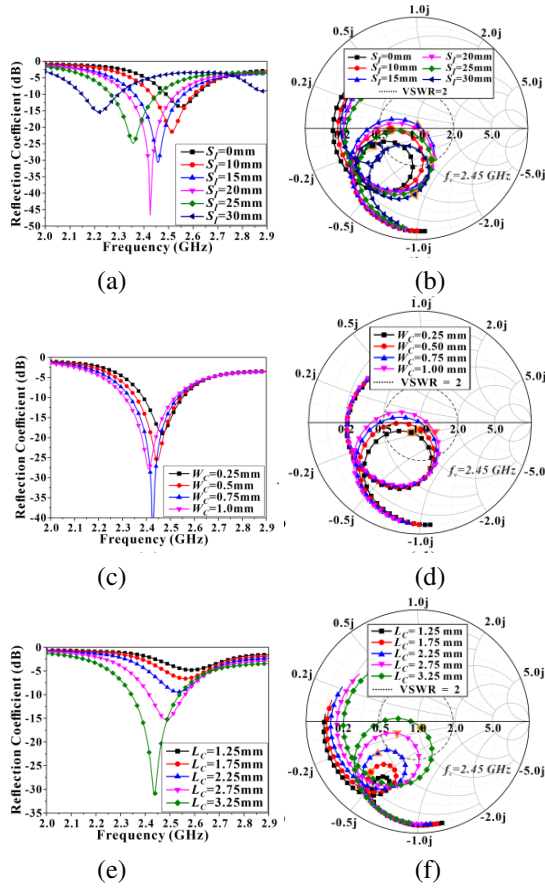
(a)   (b)

(c)   (d)

(e)   (f)

Fig. 2. Simulated reflection coefficients and impedance variations on the smith chart of the proposed antenna according to the (a)-(b) slot length (S_l), (c)-(d) width (W_c) of the capacitance feed line resonator, and (e)-(f) length (L_c) of the capacitance feed line resonator. The resonance frequency f_c = 2.45 GHz).
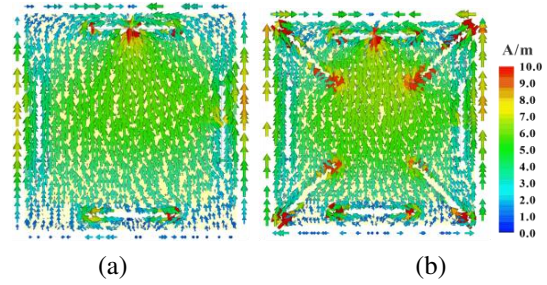

(a)   (b)

Fig. 3. Current distribution of the conventional and proposed antennas: (a) Conventional patch antenna without slots and (b) proposed patch antenna with slots.
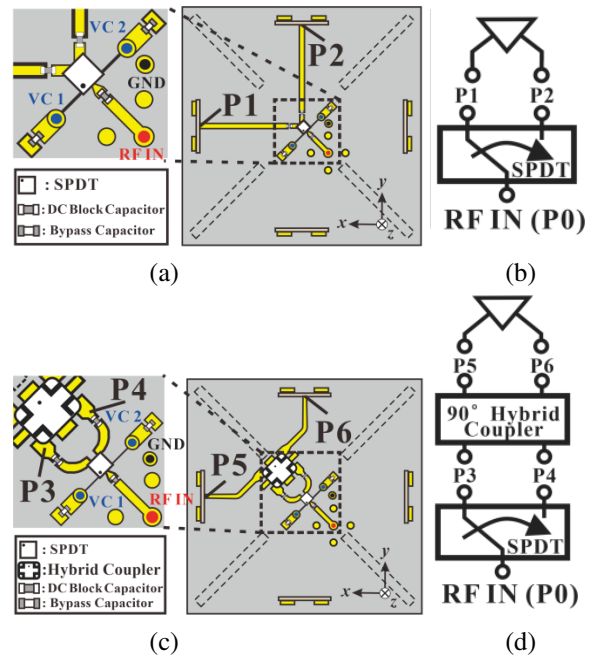

(a)   (b)

(c)   (d)

Fig. 4. Configurations and block diagram of the proposed feeding network: (a)-(b) Linear polarization modes and (c)-(d) circular polarization modes.

of the proposed antenna and the length of the slot. Figures 2 (a)-(b) show the change in resonance frequency according to the change in the length of the slot (S_l) placed on the proposed antenna ground plane. It is possible to adjust the resonance frequency up to 400 MHz by changing the length of the slot on the ground surface.

Figures 2 (c)-(f) show the simulated reflection coefficients and impedance variations of the proposed antenna according to the feed line width (W_c) and length (L_c). Figure 3 shows the current distribution of the conventional and proposed patch antennas.

For the proposed patch antenna, the slot placed at each corner will result in a longer current path than the conventional patch antenna, resulting in a longer electrical length of the patch antenna. Therefore, the ground surface slot structure reduced in size by approximately

25%. For wide bandwidth, capacitance feed lines are printed on one side of the crossed rectangular support using two RF-60 substrates, as shown in Fig. 1 (b). To match impedance while enhancing bandwidth, the length and width of the capacitance feed line are adjusted to resonate at 2.45 GHz. Figure 4 shows the four modes of polarization achieved from two cases of reconfigurable feeding networks. The linear polarization feeding network in Figs. 4 (a)-(b) comprises one input port, two output ports, and one single-pole double-throw (SPDT) switch. The SPDT switch is the CG2176X3-C2 AS179-92LF model manufactured by Skyworks. In addition, a 100 pF capacitor is connected for DC blocking, and a

1000 pF capacitor is connected for bypass. All of these capacitors are manufactured by Murata in the 01005-inch size. Figures 4 (c)-(d) show the circular polarization feeding network. The circular polarization feeding network has a configuration in which a hybrid coupler is added to the front of the output ports of the linear polarization feeding network. The polarization mode is selected by using the SPDT switch when the RF input signal is applied. The RF signal input in Figs. 4 (a)-(b) is transmitted to P1 or P2 through the SPDT switch, and the RF signal is fed to the patch through the capacitance feeding line under the patch. The patch antenna has a horizontal LP (H-LP) when the signal is applied to P1, and has the characteristics of vertical LP (V-LP) when the signal is applied to P2. On the other hand, the RF signal input in Figs. 4 (c)-(d) is transmitted to P3 or P4 through the SPDT switch, which transmits a phase difference signal to P5 and P6 through a 90° hybrid coupler so that the RF signal is fed to the patch through the capacitance feed line under the patch. The 90° hybrid coupler used in this circuit is the RCP2650Q03 from RN2 Technologies. When a signal is applied to P3 through the SPDT switch, the patch antenna is applied with a signal of 0° to P5 and a signal of 90° to P6, and the patch antenna has the left-hand CP (LHCP) mode characteristic. In this way, when a P4 signal is applied through the SPDT switch, a 90° signal is applied to the P5 and a 0° signal is applied to the P6 so that the patch antenna has the right-hand CP (RHCP) mode characteristics. Figure 5 shows the implemented and mounted proposed antenna on a UAV. Figures 5 (a)-(c) show the top and bottom views of the proposed patch antenna. Figures 5 (d)-(e) show the overall configuration and mounted proposed antenna on the UAV.

III. RESULT AND DISCUSSION

The proposed UAV antenna, along with the feeding network operating in the 2.45 GHz ISM band has been optimized using a commercial full-wave electromagnetic tool (CST Microwave Studio 2022). To miniaturize the antenna design, the proposed antenna was fabricated on an RF-60 substrate of 0.64 mm thickness and a copper thickness of 18 μm. The reflection coefficient and isolation were measured using a vector network from Rohde & Schwarz, and the radiation patterns, axial ratio, and gains for each polarization were measured by the Korea Radio Promotion Association's EM Technology Institute. The measured results of the dual LP antenna are presented in Figs. 6 (a)-(b). In the case of dual orthogonal LP in Fig. 6 (a), the reflection coefficients of H-LP and V-LP modes are less than -10 dB, and the 10-dB bandwidth of LP modes is approximately 4.9% from 2.39 GHz to
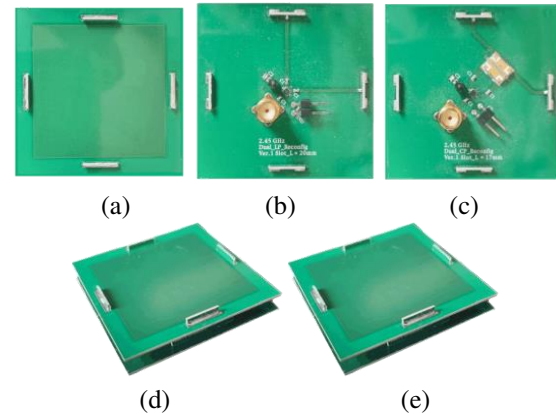

Fig. 5. Implemented and mounted proposed antenna on the UAV: (a) Top views of the patch antenna, (b)-(c) bottom views of the feeding networks, (d) overall configurations of the proposed patch antenna, and (e) mounted proposed patch antenna.

2.51 GHz. The switch's insertion loss is approximately -0.75 dB, and the isolation between two capacitance feeders is -23 dB at 2.45 GHz.

Figure 6 (b) shows the elevation radiation patterns (xz plane) for each polarization mode. They are almost the same for horizontal and vertical LP. The peak gain and front-to-back ratio are more than 6.6 dBi and 12.3 dB to 13.5 dB in each polarization mode, and the efficiencies of LP modes are approximately 82%. Figures 6 (c)-(f) show the characteristics of the dual circularly polarized antenna.

In Fig. 6 (c), the reflection coefficients of RHCP and LHCP modes are less than -10 dB, which include the insertion losses of the SPDT switch and hybrid couplers. The phase variation is approximately 90°, and the transmission coefficient, including a 3 dB divided power loss is approximately -3.5 dB. The 10 dB bandwidth of CP modes is approximately 4.5% from 2.38 GHz to 2.49 GHz. Figure 6 (d) shows the axial ratio and phase variation of the dual circularly polarized antenna. The 3-dB axial ratio bandwidths of CP modes cover approximately 12% from 2.3 GHz to 2.6 GHz. The phase variations are ±90° in each RHCP and LHCP mode.

Figures 6 (e)-(f) show the realized gain and radiation pattern. The peak gain and front-to-back ratio are 7.2 dBi and 15.7 dB to 27 dB, respectively. The performance of the proposed antenna is compared to other multi-polarized reconfigurable antennas, as indicated in Table 1. Compared to the previously reported antennas, the proposed antenna has a smaller size, wider bandwidth, and higher gain.

Table 1: Performance comparisons of multiple-polarized antennas

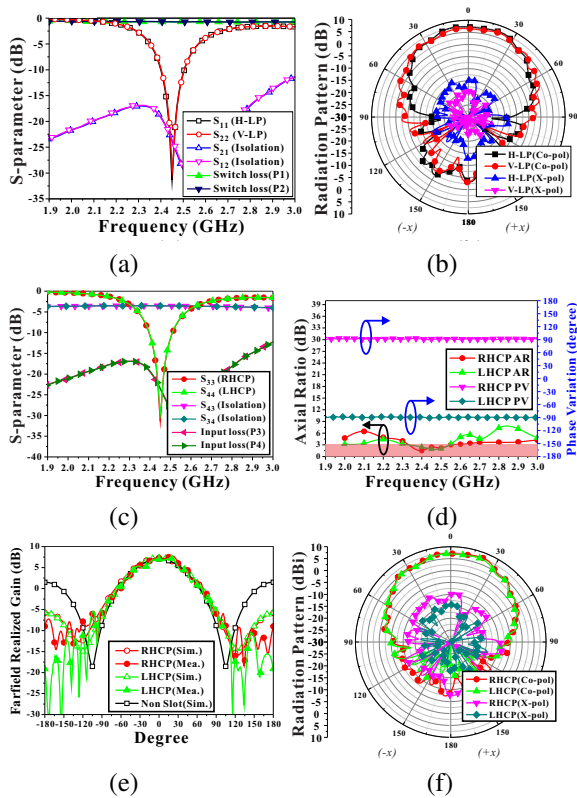| Ref.	f_c (GHz)	BW (%)	Gain (dBi)	Polarization	AR BW (%)	Elect. Size (λ_o^3)
[7]	2.46	52.03	9	1 LP & 2 CP	63.1-	0.65×0.65×0.19
[8]	2.65	34	3.7	4 LP	-	0.7×0.7×0.23
[9]	2.7	37	8.9	3 LP & 2 CP	50.6	0.68×0.68×0.24
[10]	2.45	11.4	7.3	CLP & 2 CP	14	0.64×0.64×0.05
[12]	4.805	7.28	6.63	1 LP & 2 CP	7	0.56×0.56×0.037
[14]	3.5	11.4	7.5, 5	1 LP & 2 CP	11.4	0.9×0.9×0.036
[16]	2.4	0.8	5.83, 6.4	1 LP & 2 CP	0.5	0.65×0.65×0.01
[17]	3.4	5.9	5.89, 5.81	2 LP	-	0.85×0.85×0.26
Prop.	2.45	4.5	6.6, 7.2	2 LP or 2 CP	12	0.389×0.389×0.05

Fig. 6. Characteristics of the proposed antenna at each polarization mode: (a) Measured S-parameters of a linearly polarized antenna, (b) measured radiation patterns of two LP modes in the *xz* plane, (c) measured S-parameters of the dual circularly polarized antenna, (d) axial ratio and phase variation of the dual circularly polarized antenna, (e) simulated and measured realized gain of the dual CP modes, and (f) radiation patterns of the dual CP modes in the *xz* plane.

IV. CONCLUSION

A 2.45 GHz multi-polarized reconfigurable patch antenna for U2X communications is presented in this paper. The proposed feeding network utilizes an SPDT switch and hybrid coupler to achieve various polarization types, including V-LP or H-LP, as well as LHCP or RHCP. The proposed multi-polarized reconfigurable antenna can provide a compact size and high gain in the 2.45 GHz ISM band. This antenna can be easily mounted on UAVs and has a low-profile, balanced structure. It also offers ease of control for selecting different types of polarization. Therefore, the proposed antenna can be widely used for UAV applications, making it a promising candidate for performing a diverse range of missions in numerous fields.

REFERENCES

[1] P. G. Fahlstrom, T. J. Gleason, and M. H. Sadraey, *Introduction to UAV Systems*. Hoboken, NJ: Wiley, 2022.

[2] Y. Fan, X. Liu, B. Liu, and R. Li, "A broadband dual-polarized omnidirectional antenna based on orthogonal dipoles," *IEEE Antennas Wireless Propag. Lett.,* vol. 15, pp. 1257-1260, 2016.

[3] D. Wu, L. Yang, G. Fu, and X. Shi, "Compact and low-profile omnidirectional circularly polarized antenna with four coupling arcs for UAV applications," *IEEE Antennas Wireless Propag. Lett.,* vol. 16, pp. 2919-2922, 2017.

[4] D. G. Seo, J. S. Park, and W. S. Lee, "Lightweight printed dipole antenna array with 3×2 beamforming network for wide UAV communication

coverage," *Journal of Engineering & Technology*, vol. 15, pp. 1769-1773, 2020.

[5] A. Khidre, K. Lee, F. Yang, and A. Z. Elsherbeni, "Circular polarization reconfigurable wideband E-shaped patch antenna for wireless applications," *IEEE Trans. Antennas Propag.*, vol. 61, no. 2, pp. 960-964, 2013.

[6] J.-S. Row, W.-L. Liu, and T.-R. Chen, "Circular polarization and polarization reconfigurable designs for annular slot antennas," *IEEE Trans. Antennas Propag.*, vol. 60, no. 12, pp. 5998-6002, 2012.

[7] G. Jin, L. Li, W. Wang, and S. Liao, "A wideband polarization reconfigurable antenna based on optical switches and C-shaped radiator," *Microw. Optical Technology Lett.,* vol. 62, no. 6, pp. 2415-2422, 2019.

[8] H. Wong, W. Lin, L. Huitema, and E. Arnaud, "Multi-polarization reconfigurable antenna for wireless biomedical system," *IEEE Trans. Biomed. Circuits Syst.*, vol. 11, no. 3, pp. 652-660, 2017.

[9] H. H. Tran, N. Nguyen-Trong, T. T. Le, and H. C. Park, "Wideband and multi-polarization reconfigurable crossed bowtie dipole antenna," *IEEE Trans. Antennas Propag.,* vol. 65, no. 12, pp. 6968-6975, 2017.

[10] L. Ran, D.-P. Yang, and S.-Y. Wang, "A mode-combination-based polarization-reconfigurable antenna," *Int. J. RF Microw. Comput.-Aided Eng.*, vol. 32, no. 4, 2022.

[11] K. M. Mak, H. W. Lai, K. M. Luk, and K. L. Ho, "Polarization reconfigurable circular patch antenna with a C-shaped," *IEEE Trans. Antennas Propag.*, vol. 65, no. 3, pp. 1388-1392, 2017.

[12] M. Li, Z. Zhang, and M.-C. Tang, "A compact, low-profile, wideband, electrically controlled, tri-polarization-reconfigurable antenna with quadruple gap-coupled patches," *IEEE Trans. Antennas Propag.*, vol. 68, no. 8, pp. 6395-6400, 2020.

[13] S. Chen, F. Wei, P. Qin, Y. J. Guo, and X. Chen, "A multi-linear polarization reconfigurable unidirectional patch antenna," *IEEE Trans. Antennas Propag.*, vol. 65, no. 8, pp. 4299-4304, 2017.

[14] H. L. Zhu, S. W. Cheung, X. H. Liu, and T. I. Yuk, "Design of polarization reconfigurable antenna using metasurface," *IEEE Trans. Antennas Propag.,* vol. 62, no. 6, pp. 2891-2898, 2014.

[15] C. Y. D. Sim, Y. J. Liao, and H. L. Lin, "Polarization reconfigurable eccentric annular ring slot antenna design," *IEEE Trans. Antennas Propag.,* vol. 63, no. 9, pp. 4152-4155, 2015.

[16] X.-X. Yang, B.-C. Shao, F. Yang, A. Z. Elsherbeni, and B. Gong, "A polarization reconfigurable patch antenna with loop slots on the ground plane," *IEEE Antennas Wireless Propag. Lett.,* vol. 11, pp. 69-72, 2012.

[17] Y. Mu, J. Han, D. Xia, X. Ma, H. Liu, and L. Li, "The electronically steerable parasitic patches for dual-polarization reconfigurable antenna using varactors," *Applied Computational Electromagnetics Society (ACES) Journal*, pp. 58-67, 2022.

Seong-Hyeop Ahn received the B.S. and M.S. degrees in electronic engineering from Gyeongsang National University (GNU), Jinju, South Korea, in 2018 and 2020, respectively. Since 2022, he has been working toward the Ph.D. degree in electronic engineering from GNU.

His research interests are high-power microwave systems, near-field wireless power transfer and communications systems, RFID/IoT sensors, and RF/microwave circuit and antenna designs.

Yu-Seong Choi received the B.S. and M.S. degrees in electronic engineering from Gyeongsang National University (GNU), Jinju, South Korea, in 2019 and 2021, respectively. Since 2022, he has been working in Korea Aerospace Industries.

His research interests include reconfigurable antenna design & analysis, RF/Microwave circuits and systems, and RFID/IoT sensors.

Mohamed Elhefnawy received the B.S. and M.S. degrees in electronics and communications engineering from Tanta University and Arab Academy for Science & Technology, Egypt, in 1999 and 2005, respectively. He received a Ph.D. degree in communications engineering from USM University, Malaysia, in 2010. Since 2023, he has been working as a senior researcher in the Department of Electronic Engineering, Gyeongsang National University (GNU), Jinju, South Korea. From 2012 to 2023, he worked as a lecturer in the Department of Electrical Engineering at the Faculty of Engineering, October 6 University, Egypt.

He has a strong academic background that includes RF/microwave engineering, electromagnetic theory, and antenna theory. His research interests include antennas, wave propagation, RF and microwave, and communications.

Wang-Sang Lee received the B.S. degree from Soongsil University, Seoul, South Korea, in 2004, and the M.S. and Ph.D. degrees in electrical engineering from the Korea Advanced Institute of Science and Technology (KAIST), Daejeon, South Korea, in 2006 and 2013, respectively.

From 2006 to 2010, he was with the Electromagnetic Compatibility Technology Center, Digital Industry Division, Korea Testing Laboratory (KTL), Ansan-si, South Korea, where he was involved in the international standardization for radio frequency identification (RFID) and photovoltaic systems as well as electromagnetic interference (EMI)/EMC analysis, modeling, and measurements for information technology devices. In 2013, he joined the Korea Railroad Research Institute (KRRI), Uiwang-si, South Korea, as a Senior Researcher, where he was involved in the position detection for high-speed railroad systems and microwave heating for low-vibration rapid tunnel excavation systems. Since 2014, he has been an Associate Professor with the Department of Electronic Engineering, Gyeongsang National University (GNU), Jinju, South Korea. From 2018 to 2019, he was a Visiting Scholar with the ATHENA Group, Georgia Institute of Technology, Atlanta, GA, USA. His current research interests include near- and far-field wireless power and data communications systems, RF/microwave antenna, circuit, and system design, RFID/Internet of Things (IoT) sensors, and EMI/EMC.

Dr. Lee is a member of IEEE, IEC/ISO JTC1/SC31, KIEES, IEIE, and KSR. He was a recipient of the Best Paper Award at IEEE RFID in 2013, the Kim Choong-Ki Award Electrical Engineering Top Research Achievement Award at the Department of Electrical Engineering, KAIST, in 2013, the Best Ph.D. Dissertation Award at the Department of Electrical Engineering, KAIST, in 2014, the Young Researcher Award at KIEES in 2017, and the Best Paper Awards at IEIE in 2018 and KICS in 2019.